Life Sciences in Space Research 13 (2017) 1–11

Contents lists available at ScienceDirect

Life Sciences in Space Research

journal homepage: www.elsevier.com/locate/lssr

Predictions of space radiation fatality risk for exploration missions

Francis A. Cucinotta*, Khiet To, Eliedonna Cacao

Department of Health Physics and Diagnostic Sciences, University of Nevada, Las Vegas, NV, United States of America

ARTICLE INFO

Article history:
Received 15 December 2016
Accepted 31 January 2017

Keywords:
Galactic cosmic rays
Heavy ions and high LET radiation
Cancer and circulatory disease risk
Relative biological effectiveness
Quality factors

ABSTRACT

In this paper we describe revisions to the NASA Space Cancer Risk (NSCR) model focusing on updates to probability distribution functions (PDF) representing the uncertainties in the radiation quality factor (QF) model parameters and the dose and dose-rate reduction effectiveness factor (DDREF). We integrate recent heavy ion data on liver, colorectal, intestinal, lung, and Harderian gland tumors with other data from fission neutron experiments into the model analysis. In an earlier work we introduced distinct QFs for leukemia and solid cancer risk predictions, and here we consider liver cancer risks separately because of the higher RBE's reported in mouse experiments compared to other tumors types, and distinct risk factors for liver cancer for astronauts compared to the U.S. population. The revised model is used to make predictions of fatal cancer and circulatory disease risks for 1-year deep space and International Space Station (ISS) missions, and a 940 day Mars mission. We analyzed the contribution of the various model parameter uncertainties to the overall uncertainty, which shows that the uncertainties in relative biological effectiveness (RBE) factors at high LET due to statistical uncertainties and differences across tissue types and mouse strains are the dominant uncertainty. NASA's exposure limits are approached or exceeded for each mission scenario considered. Two main conclusions are made: 1) Reducing the current estimate of about a 3-fold uncertainty to a 2-fold or lower uncertainty will require much more expansive animal carcinogenesis studies in order to reduce statistical uncertainties and understand tissue, sex and genetic variations. 2) Alternative model assumptions such as non-targeted effects, increased tumor lethality and decreased latency at high LET, and non-cancer mortality risks from circulatory diseases could significantly increase risk estimates to several times higher than the NASA limits.

1. Introduction

Fatality risks for cancer and other diseases due to occupational exposure are a concern for astronauts on long-term space exploration missions where galactic cosmic rays (GCR) and secondary radiation — made up predominantly of high-energy protons, high-energy and charge (HZE) nuclei and neutrons, and possible solar particle events (SPEs) — comprised largely of low- to medium-energy protons will lead to significant organ doses. NASA limits the risk of exposure induced death (REID) due to cancer to no more than a 3% probability at a 95% confidence level (NCRP, 2014). NASA has followed recommendations from the National Council of Radiation Protection and Measurements (NCRP) for setting radiation dose limits (NCRP, 2000; NCRP, 2014). The importance of uncertainties in estimating space radiation risks have been recognized by several reports from the NCRP (NCRP, 1997; NCRP, 2006) and National Research Council (NRC) (NRC, 2013). In 1996 the National Academy of Sciences Space Science Board estimated a 5–10-fold uncertainty for deep space cancer fatality risks (NAS, 1996), while more recent estimates suggest about a 3-fold uncertainty (Cucinotta 2015). There are no epidemiology data for late effects from GCR other than cataracts (Cucinotta et al., 2001; Chylack et al., 2009), while important lifestyle differences in the astronaut compared to other populations occur (Cucinotta et al., 2013a; Cucinotta et al., 2016a). Uncertainties in space radiation risk estimates are dominated by lack of information on the radiobiology of HZE particles that produce both quantitative and qualitative differences in biological effects compared to γ-rays or x rays.

In previous work (Cucinotta et al., 2013a, 2013b) we proposed a new model to estimate space radiation cancer risk that was reviewed by the NRC (NRC, 2013) with further review by the NCRP (2014), resulting in the NASA Space Cancer Risk (NSCR) model-2012 (Cucinotta et al., 2013a). Radiation quality factors (QFs) and

* Correspondence author.
E-mail address: francis.cucinotta@unlv.edu (F.A. Cucinotta).

http://dx.doi.org/10.1016/j.lssr.2017.01.005

dose-rate modifying factors, such as the dose and dose-rate reduction effectiveness factor (DDREF), are variables used to scale human epidemiology data for low LET radiation at high dose-rate to the protons, heavy ions and secondary radiation in chronic GCR exposures. Features of the NSCR model include QFs based on track structure concepts with distinct QFs for leukemia and solid cancer risks, a never-smoker model to represent baseline cancer and non-cancer disease risks for astronauts, and use of a cancer incidence to mortality risk transfer methodology. Probability distribution functions (PDFs) for estimating uncertainties in each model parameter were formulated while performing Monte-Carlo sampling over each PDF to estimate an overall REID uncertainty.

Microscopic energy deposition by protons and heavy ions can be described by a track core term representing the direct ionization and excitations of target molecules by primary particles and low energy secondary electrons produced through ionization called δ-rays, and a penumbra term representing the diffuse energy deposition by higher energy δ-rays of low LET, which may extend for 100′s of microns from a particle track for relativistic particles. More recently the QFs used in the NSCR model were revised to further consider track core and penumbra effects in proton and heavy ion exposures (Cucinotta, 2015; Cucinotta et al., 2015). Based on experimental observations for high LET irradiation, no dose-rate modification was applied to the core term, which reduced the overall uncertainties and risk estimates by more than 25% for GCR.

Bayesian analysis has been used to estimate the probability distribution function representing the uncertainty in the DDREF using a prior distribution estimated from the Atomic-bomb survivor data and a likelihood function from certain mouse tumor studies with γ-rays (NAS, 2006). In our previous work we noted that values of RBE's and DDREF's are correlated and therefore estimated model parameters from experiments of mouse solid tumors where both parameters were determined, which formed the basis for our DDREF uncertainty analysis. More recently the BEIR VII reports recommendation of a DDREF of 1.5 has been challenged by Hoel (2015) who shows why the BEIR VII subjective assumptions related to dose truncation of the Japanese atomic-bomb survivors dose response for solid cancer risk are faulty, and suggests that a DDREF of 2 or more is supported by improved analysis. Use of a DDREF of 2 in radiation protection is recommended by the International Commission of Radiological Protection (2007) and the NCRP (2000).

In this paper we present new estimates of probability distribution functions (PDF) representing uncertainties in QF parameters and describe risk predictions for 1-year ISS and space exploration missions. We revise estimates of the QF parameters by analyzing data from cell surrogate endpoints with heavy ions (Cacao et al., 2016), and mouse tumor induction studies with fission neutrons and heavy ions, including recent studies of colorectal and intestinal tumors (Suman et al., 2016) and Harderian gland tumors (Chang et al., 2016). We consider alternatives to the DDREF analysis of the BEIR VII report (NAS, 2006) suggested by Hoel (2015). In addition we augment our previous likelihood function that enters into the Bayesian analysis based on mouse solid tumor data for γ-rays with DDREF estimates from high-energy proton experiments with surrogate cancer endpoints that directly compared high to low dose-rate. The energy distribution of δ-rays from protons is more similar to those of GCR than ^{60}Co γ-rays, however our analysis shows that DDREF from proton experiments are very similar to those found for mouse tumor induction studies with γ-ray irradiations. We also discuss alternative risk assessment assumptions, including higher tumor lethality at high LET, the inclusion of circulatory disease risks, and non-targeted effects. The resulting models are used to make predictions for a 940-day Mars mission and 1-year ISS missions, and the prospects for reducing uncertainties discussed.

2. Methods

2.1. Cancer risk projection model

We briefly summarize recent methods developed to predict the risk of exposure induced death (REID) for space missions and associated uncertainty distributions (Cucinotta et al., 2013a; Cucinotta et al., 2015). The instantaneous cancer incidence or mortality rates, $\lambda_{\rm I}$ and $\lambda_{\rm M}$, respectively, are modeled as functions of the tissue averaged absorbed dose D_T, or dose-rate D_{Tr}, gender, age at exposure a_E, and attained age a or latency L, which is the time after exposure until cancer occurrence or death, $L = a - a_{\rm E}$. The $\lambda_{\rm I}$ (or $\lambda_{\rm M}$) is a sum over rates for each tissue that contributes to cancer risk, $\lambda_{\rm IT}$ (or $\lambda_{\rm MT}$). The total risk of exposure induced cancer (REIC) is calculated by folding the instantaneous radiation cancer incidence-rate with the probability of surviving to time t, which is given by the survival function $S_0(t)$ for the background population times the probability for radiation cancer death at previous time, summing over one or more space mission exposures, and then integrating over the remainder of a lifetime, which is taken as 100 years in calculation:

$$REIC(a_{\rm E}, D_{\rm T}) = \sum_{j=1}^{N_m} \int_{a_{{\rm E}j}}^{100} dt \lambda_{Ij}(a_{{\rm E}_j}, t, D_{{\rm T}j}) S_0(t) e^{-\sum_{k=1}^{N_m} \int_{a_E}^{t} dz \lambda_{M_k}(a_{{\rm E}_k}, z, D_{{\rm T}_k})} \quad (1)$$

where z is the dummy integration variable. In Eq. (1), N_m is the number of missions (exposures), and for each exposure, j, there is a minimum latency of 5-years for solid cancers, and 2-years for leukemia assumed. Tissue specific REIC estimates are similar to Eq. (1) using the single term from $\lambda_{\rm I}$ of interest. The equation for REID estimates is similar to Eq. (1) with the incidence rate replaced by the mortality rate (defined below).

The tissue and sex-specific cancer incidence rate for an organ absorbed dose, $D_{\rm T}$, is written as a weighted average of the multiplicative and additive transfer models, denoted as a mixture model. However, a scaling factor, R_{QF} is introduced for extrapolating to low dose and dose-rates and estimating the radiation quality dependences of cancer risk for a particle of charge number Z and kinetic energy per nucleon, E:

$$\lambda_{I{\rm T}}(a_{\rm E}, a, D_{\rm T}, Z, E) = [\nu_{\rm T} ERR_{\rm T}(a_{\rm E}, a)\lambda_{0I{\rm T}}(a) + (1-\nu_{\rm T}) EAR_{\rm T}(a_{\rm E}, a)] R_{QF}(Z, E) D_{\rm T} \quad (2)$$

where $\nu_{\rm T}$ is the tissue-specific transfer model weight, $\lambda_{0I{\rm T}}$ is the tissue-specific cancer incidence rate in the reference population, and where $ERR_{\rm T}$ and $EAR_{\rm T}$ are the tissue specific excess relative risk and excess additive risk per Sievert, respectively, with values from the United Nations report (UNSCEAR, 2008). The sex and tissue specific rates for cancer mortality $\lambda_{M{\rm T}}$ are modeled following the BEIR VII report (NAS, 2006) whereby the incidence rate of Eq. (2) is scaled by the age, sex, and tissue specific ratio of rates for mortality to incidence in the population under study in terms of a sex dependent tissue dose equivalent, $H_{\rm T}$:

$$\lambda_{M{\rm T}}(a_{\rm E}, a, H_{\rm T}) = \frac{\lambda_{0M{\rm T}}(a)}{\lambda_{0I{\rm T}}(a)} \lambda_{I{\rm T}}(a_{\rm E}, a, H_{\rm T}) \quad (3)$$

Background cancer, circulatory and pulmonary disease rates that enter the model are updated from our earlier publication (Cucinotta 2015; Cucinotta et al., 2015) using Devcan software (Devcan, 2007) and recent National Cancer Institute (NCI) and Center of Disease Control (CDC) WONDER data bases for the U.S. population (SEER, 2015; CDC, 2015).

R_{QF} is estimated using RBE's determined from low dose and dose-rate particle data relative to acute γ-ray exposures for doses of about 0.5–3 Gy, which we denote as RBE$_{\gamma\rm Acute}$. This approach

alleviates the need to consider low dose-rate γ-ray experiments for RBE estimates, however for low LET particles a DDREF is still warranted because of their expected reduced effectiveness at low dose-rates compared to acute γ-ray exposures at higher doses. The scaling factor in Eq. (2) is then written:

$$R_{QF}(E,Z) = \frac{Q_{low}(Z,E)}{DDREF} + Q_{high}(Z,E) \quad (4)$$

A key assumption of the model given by Eq. (4) is that the low ionization density part of a particle track is influenced by dose-rate effects as represented by the first term on the right hand side of Eq. (4), while the high ionization density part of a particles track has no dependence on dose-rate as described by the second term on the right-hand side of Eq. (4). A DDREF is needed for the low ionization density particles or track regions because model parameters are largely derived from radiobiological data at higher doses and dose-rates than those occurring in space.

The low and high ionization density track contributions are parameterized as:

$$Q_{low}(Z,E) = (1 - P(Z,E)) \quad (5)$$

and

$$Q_{high}(Z,E) = \frac{(\Sigma_0/\alpha_\gamma)P(Z,E)}{L} \quad (6)$$

respectively, where L is the LET, the ratio (Σ_0/α_γ) is treated as a single parameter, and the function originating in the parametric model of Katz (Katz et al., 1971) is given by,

$$P(Z,E) = \left(1 - e^{-Z^{*2}/\kappa\beta^2}\right)^m (1 - e^{-E/0.1}) \quad (7)$$

The second product in Eq. (7) represents a so-called thin-down correction for low energy particles (Cucinotta et al., 2013a). The values of shape parameters m and κ are described below. In this approach there are two physical parameters: particle charge number, Z and kinetic energy per atomic mass unit, E. However, a key parameter that describes the density of a particle track is Z^{*2}/β^2, where Z^* is the effective charge number of a particle, which includes a velocity-dependent screening correction at low energies, and β is the particle velocity scaled to the speed of light. The effective charge formula of Barkas is used (Barkas, 1963) as described below. The LET for protons and helium in tissue are calculated using the National Institute of Standards (NIST, 2009) data base using effective charge to scale the LET of heavy ions to protons.

A distinct scaling, R_{QF} is used for estimating solid cancer and leukemia risks (Cucinotta et al., 2013a) based on estimates of smaller RBEs for acute myeloid leukemia and thymic lymphoma in mice compared to those found for solid cancers for fission neutrons (Ullrich and Preston, 1987) and heavy ions (Weil et al., 2009; 1014). Also studies of leukemia risk in thorotrast patients suggest a low RBE at high LET (Boice, 1993).

2.2. Model parameters and PDF's of parameter uncertainty

There are four parameters appearing in the function R_{QF}: (Σ_0/α_γ), m, κ, and DDREF. For each of these parameters central values (most likely) and PDFs representing uncertainty in these values are formulated based on available experimental data. In the current effort we note that the relationship between estimates of (Σ_0/α_γ) based on reported RBE values is dependent on the values of m and κ assumed, and we consider this relationship in parameter estimates from heavy ion and fission neutron experiments.

Our previous publication (Cacao et al., 2016) provides comprehensive estimates of the values of m and κ for cancer risk surrogate endpoints of gene mutation, chromosomal aberrations, and neoplastic transformation for experiments with heavy ions. For the best fitting value of biological action cross section slope parameter, $m = 3$, we found a mean and standard deviation (SD), $\kappa = 534 \pm 65$ which is very close to a previous subjective estimate of $\kappa = 525$ (Cucinotta et al., 2013a). A recent estimate of these parameters for the Harderian gland experiments has been made (Cucinotta and Cacao, 2016), which provides an estimate of $\kappa = 713 \pm 121$ in a targeted effects model. These data sets were averaged with equal weight given to the Harderian gland experiment and the combined cell culture surrogate endpoint experiments to estimate an overall value for heavy ions of $\kappa = 624 \pm 69$. For protons and helium we assume $\kappa = 1000$ with a SD = 250 based on review of studies (Cucinotta et al., 2013a) with low energy protons, helium ions, and neutrons (Belli et al., 1992; Thacker et al., 1979; Tracy et al., 2015; Miller and Hall, 1991; Pandita and Geard, 1996; Tanaka et al., 1999). For the PDF of the action cross section slope parameter, m, we assume a normal distribution with mean of 3 and SD of 0.5. Values of κ for $m \neq 3$ were determined by conditional Monte-Carlo sampling using $\kappa(m) = 4\kappa(m=3)/(m+1)$ as described previously (Cucinotta et al., 2013a).

Using $m = 3$, the value of (Σ_o/α_γ) was estimated while sampling from the model dependent PDF for κ for both particle radiation and fission neutron using the $RBE_{\gamma Acute}$ experimental data shown in Table 2. In this manner, (Σ_o/α_γ) was estimated using Eq. (8), which is derived from Eq. (4):

$$(\Sigma_0/\alpha_\gamma) = \frac{RBE_{\gamma acute}L}{P} - \frac{(1-P)}{P}\frac{L}{DDREF} \quad (8)$$

We used a DDREF value of 2 in these estimates; however we note the second term on the right-hand side of Eq. (8) is much smaller than the first-term for high LET irradiations, which reduces the influence of the value of the DDREF assumed.

To estimate (Σ_o/α_γ) values from experiments with fission neutrons, the absorbed dose from charged particles produced by fission neutrons was first determined using:

$$D_{fn} = c \int dE \qquad \phi_p(E)L(E) \quad (9)$$

where $\phi_p(E)$ is the charged particle fluence spectrum based on published data of Edwards and Dennis (1975), c is a constant, and $L(E)$ is the LET in skeleton muscle. Using the energy dependent fluence of charged particles produced by fission neutrons, $RBE(E)$ at different (Σ_o/α_γ) over a range of κ values being considered were calculated using Eq. (4), and then the dose-averaged RBE was computed as:

$$\overline{RBE} = \frac{\int dE\phi_P(E)RBE(E)L(E)}{\int dE\phi_P(E)L(E)} \quad (10)$$

Fig. 1 shows proton energy spectra from fission neutrons, and the energy dependent RBE for, which is used to estimate values of (Σ_o/α_γ) using $\kappa = 1000$. Protons dominate the fission neutron biological effects, and contributions from heavy ion elastic recoils and γ-rays to the dose-averaged RBE were estimated to be small (< 5%) (Edwards and Dennis, 1975) and not considered in the analysis. $\overline{RBE}$ was then compared directly to experiments by Ullrich and co-workers (Ullrich et al., 1976; Ullrich and Storer, 1979; Ullrich 1983; Ullrich 1984) and Grahn et al. (1992) to estimate (Σ_o/α_γ).

2.3. Data fitting

All statistical analysis and data fitting were done using STATA/SE version 14.1 (Stata Corp.). Log-normal distribution fitting by maximum likelihood is based on Stata module "lognfit" (Jenkins, 2013). CDF's were fitted to the data of Table 3 using SigmaPlot version 12.5 considering several distributions including Logistic, Weibull and Gompertz functions, which were tested to reach an analytic representation for Monte-Carlo sampling of the overall risk uncertainty.

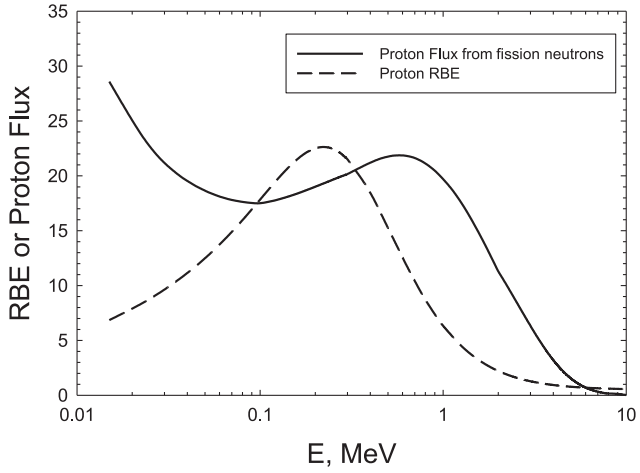

Fig. 1. Estimates of proton energy spectrum (arbitrary units) from ^{252}Cf fission neutrons by Edwards and Dennis (1975) and energy dependent relative biological effectiveness factor (RBE) for solid cancer risk in track structure model described in the text with parameters m = 3, $\kappa = 1000$, and $\Sigma_0/\alpha_\gamma = 2500\mu m^2$ Gy.

2.4. Circulatory disease risk estimates

As described previously (Cucinotta et al., 2013b) we use the result of the meta-analysis of several human cohorts exposed to low LET radiation (Little et al., 2012) to estimate circulatory disease mortality risks. For circulatory disease risk estimates, information on RBE's for protons and HZE particles and secondary radiation are even sparser than those related to cancer risks. For our central estimates we use the RBE's recommended for non-cancer effects (NCRP, 2000). A DDREF is not applied for circulatory disease risks because the meta-analysis of Little et al. (2012) is based to a large extent on low dose-rate (chronic) exposures to radiation workers, which were fitted with a linear dose response model. The risks of ischemic heart disease (IHD) and cerebrovascular diseases (CVD) were then considered as alternative REID predictions from those of cancer alone (Cucinotta et al., 2013b). We considered several choices for the tissue shielding for the circulatory system, including doses to the blood forming organ (BFO) system, heart, or brain. However, for GCR only modest differences occur and we used the BFO for REID estimates.

2.5. Applications to space mission assessments

For the application of the NSCR model to space mission predictions, the energy spectra for each particle type, j of LET, $L_j(E)$ for each tissue, T contributing to cancer risk denoted as $\phi_{jT}(E)$ is estimated from radiation transport codes. The particle energy spectra are folded with R_{QF} to estimate tissue specific REIC or total REID values (Cucinotta et al., 2015). For calculations for a fluence $\phi_T(Z,E)$ and absorbed dose, $D_T(Z,E)$ of a particle type described by Z and E, Eq. (2) is replaced by

$$\lambda_{ZI}(F_T, a_E, a) = \lambda_{\gamma I}(a_E, a)\left\{D_T(Z,E)\frac{(1-P(Z,E))}{DDREF} + (\Sigma_0/\alpha_\gamma)P(Z,E)\phi_T(Z,E)\right\} \quad (11)$$

where $\lambda_{\gamma I}$ is the inner bracketed terms in Eq. (2) that contains the ERR and EAR functions for individual tissues. As described previously (Cucinotta et al., 2015) calculations are made using models of the GCR environments and radiation transport in spacecraft materials and tissue, which estimate the particle energy spectra, $\phi_j(E)$ for 190 isotopes of the elements from $Z = 1$ to 28, neutrons, and dose contributions from pions, electrons and gamma-rays.

The fluence spectra, $F(X_{tr})$ where $X_{tr} = Z^{*2}/\beta^2$ can be found by transforming the energy spectra, $\phi_j(E)$ for each particle, j of mass number and charge number, A_j and Z_j respectively as:

$$F(X_{tr}) = \sum_j \left(\frac{\partial X_{tr}}{\partial E}\right)^{-1} \phi_j(E) \quad (12)$$

where we evaluate the Jacobian in Eq. (12) using the Barkas (1963) form for the effective charge number given by

$$Z^* = Z(1 - e^{-125\beta/Z^{2/3}}) \quad (13)$$

The tissue specific cancer incidence rate for GCR or SPEs can then be written as:

$$\lambda_{IT} = \lambda_{I\gamma}\left\{\sum_j \int dE\phi_{jT}(E)L_j(E)\frac{(1-P(X_{tr}))}{DDREF} + (\Sigma_0/\alpha_\gamma)\int dX_{tr}F(X_{tr})P(X_{tr})\right\} \quad (14)$$

3. Results and discussion

3.1. DDREF model and uncertainty distribution

Bayesian analysis was used to model the PDF of uncertainty in the DDREF parameter for solid cancer risk estimates in a manner similar to that used in the BEIR VII report (NAS, 2006) were a prior distribution was estimated from the curvature in the Japanese Life-Space Study (LSS) and the likelihood function from radiobiology data. We denote as Model A the prior distribution from the BEIR VII Report estimate for the LSS study using a log-normal distribution with a DDREF = 1.3 and 95% confidence intervals (CI) of [0.8, 1.9]. Recently Hoel (2015) has argued that due to subjective assumptions made in the BEIR VII report a mean DDREF of 1.3 is found, while an analysis that considers a distinct dose range from the LSS data or one that includes downward curvature at higher doses due to cell sterilization effects finds a DDREF of 2 or more. Following Hoel's analysis we used in Model B a mean DDREF of 2; however uncertainties in this value were not modeled by Hoel. Here we assume a log-normal distribution with 90% confidence intervals of [1.2, 3] as a prior distribution for Model B based on the bounds described by Hoel (2015).

In our previous report we considered DDREFs from mouse solid tumor studies data where both γ-ray and high LET radiation were available. These data were used as the likelihood function for the Bayesian analysis as shown in Fig. 2 (upper panel). We did not consider ovarian cancer and leukemia mouse data that was used by BEIR VII as appropriate for this analysis (Cucinotta, 2015). More recent experiments on heavy ion induction of colorectal and intestinal tumors (Suman et al., 2016) in mice did not provide other data to modify this aspect of the PDF of uncertainty for the DDREF because the γ-ray components of these experiments were limited, while dose responses for γ-rays in the recent Harderian gland experiments (Chang et al., 2016) were consistent with earlier data (Fry et al., 1985; Alpen et al., 1993).

Values of DDREF's estimated from high-energy proton experiments are of interest because the energy spectra of δ-rays more closely represent that of GCR compared to ^{60}Co γ-rays (Cucinotta et al., 2016b). We also surveyed published proton radiobiology data for tumors in animals and surrogate endpoints in cell culture models. Here we considered data comparing acute to low dose-rates, and analysis of curvature in acute dose response data to estimate a DDREF. We found that tumor induction studies in rhesus monkeys (Wood, 1991), RFM mice (Clapp et al., 1974), and mammary tumors in Sprague-Dawley rats (Dicello et al., 2004) did not consider a sufficient number of dose groups to estimate curvature and

Table 1
Dose and dose-rate reduction effectiveness factor (DDREF) estimates from proton experiments with surrogate cancer endpoints comparing high dose-rate (HDR) to low dose rate (LDR) exposures. Standard deviations of values are shown in parenthesis.

Endpoint	Proton Energy, MeV	α-LDR, Gy^{-1}	α-HDR, Gy^{-1}	DDREF
Aprt Mutations (*in vitro*) B6D2F1 Mouse Kidney cells	1000	6.7×10^{-5} (2.1×10^{-5})	1.53×10^{-4} (1.8×10^{-5})	2.28 (0.76)
Aprt Mutations (*in vivo*) B6D2F1 Mouse Kidney cells	1000	2.1×10^{-4} (2.6×10^{-5})	4.78×10^{-4} (4.4×10^{-5})	2.23 (0.34)
Simple Exchanges Human Lymphocytes	250	0.01504 (0.0066)	0.0335 (0.0019)	2.23 (0.99)
Simple Exchanges $ATM^{+/+}$ Fibroblasts	50, 1000	0.068 (0.006)	0.157 (0.011)	2.31 (0.26)
Simple Exchanges $ATM^{+/-}$ Fibroblasts	50, 1000	0.072 (0.004)	0.154 (0.066)	2.14 (0.15)
Neoplastic transformation of primary human fibroblasts per 10^5 survivors	100	100.47 (11.29)	271 (19.8)	2.7 (0.36)
Neoplastic transformation of primary human fibroblasts per 10^5 survivors	1000	76.8 (11.84)	342.7 (53.4)	4.46 (0.98)
Average (SD)				**2.62 (0.24)**

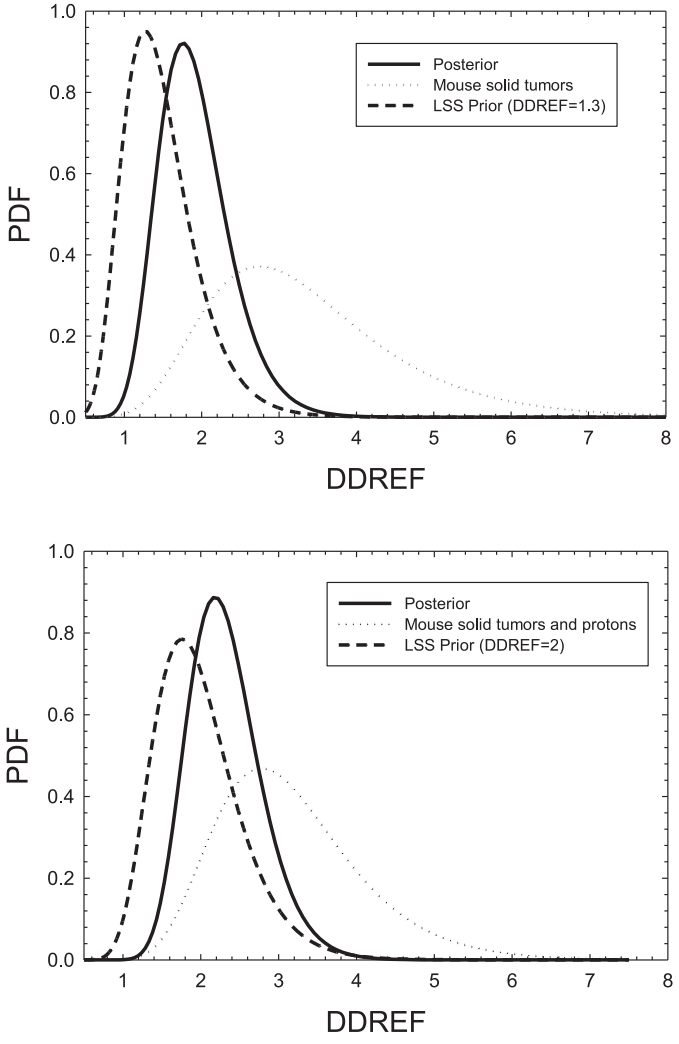

Fig. 2. Bayesian analysis of probability distribution function (PDF) for the dose and dose-rate reduction effectiveness factor (DDREF) . Upper panel uses prior distribution from the Japanese atomic-bomb lifespan study (LSS) estimated by NAS, 2006 with mean DDREF of 1.3 and likelihood function from mouse solid tumor studies with γ-rays. Lower panel uses mean DDREF of 2 as described in text for LSS study for the prior distribution, and likelihood function with mouse solid tumor studies with γ-rays and dose-rate studies for protons in surrogate cancer risk endpoints.

possible DDREF values. In cell experiments several studies comparing high dose-rate to low dose-rates have been reported, including studies of chromosomal aberration in human lymphocytes (George et al., 2002) and fibroblast cells (Peng et al., 2012), *in-vivo* and *in-vitro* studies of APRT mutations in mouse kidney epithelial cells (Kronenberg et al., 2013), and neoplastic transformation in human fibroblast cells (Stisova et al., 2011) (Table 1). DDREF estimates from proton experiments varied from 2.14 to 4.46 and strongly overlapped with estimates from solid cancers in mice exposed to acute and chronic doses of γ-rays. Fig. 2 (lower panel) shows the resulting PDF of the DDREF uncertainty in Model B which can be compared to our earlier publication for Model A (Cucinotta, 2015). For this comparison the APRT mutation estimate from *in-vivo* but not *in-vitro* experiments was used in order to avoid over-counting its weight to the likelihood function.

3.2. Quality factor parameters uncertainty

Track structure dependent parameters were estimated in our recent report for the Harderian gland experiments (Cucinotta and Cacao, 2016) based on the combined experiments of Fry et al. (1985), Alpen et al. (1993) and Chang et al. (2016) using female B6CF1 mice. For intestinal and colorectal tumors in male and female $APC^{1638N/+}$ mice we analyzed RBE's based on the dose response data reported by Suman et al. (2016). In this experiment no initial slope was found for colorectal tumors in female mice and here we scaled heavy ion data to the data from their 2 Gy γ-ray experiment. This approach yielded RBEs consistent with estimates based on ratios of linear slopes for the other tumor types in males and females as shown in Table 2. Intestinal tumors induced by fission neutrons have been studied by Ellender et al. (2011); however detailed RBE values were not reported by the authors. RBE estimates for the neutron components in the atomic bomb detonations in Hiroshima and Nagasaki, Japan carry large uncertainties with estimates from 0 to 200 appearing in the scientific literature (Cullings et al., 2014; Hunter and Charles, 2002; Little, 1997; Walsh, 2013). These estimates are based largely on organ dose estimates, while the NSCR approach would require estimates of neutron energy spectra at different tissues to consider comparisons with RBE estimates from mouse tumor induction studies.

The Harderian gland studies are the only experiments for tumor induction were a sufficient number of radiation types were used to estimate the radiation quality shape parameters, m and κ. However the value of (Σ_0/α_γ) can be estimated from experiments employing high LET irradiations if they were performed with particles near the saturation point of the biological action cross section which reduces the dependence of the estimate on the values of m and κ, such as studies with fission neutrons and heavy ions of particular kinetic energy per u, E and charge number, Z. We note that published solid tumors studies with fission neutrons or heavy ions with specific charge number, Z and kinetic energy, E do not necessarily reflect the most biologically effective particle type that may occur. For example a hypothetical study with uniform tissue irradiation by mono-energetic protons of low energy ($\sim$ 0.3 MeV) is predicted to be more effective than a ^{252}Cf fission neutron source where a mix of proton energies up to 5 MeV dominate doses, with small dose contributions from other recoil particles and γ-rays occur. In a similar manner, compared to 1 GeV/u ^{56}Fe particles a particle of lower Z and E could have a higher biological effectiveness.

Table 2
Estimates of relative biological effectiveness (RBE) from experiments of Suman et al. paper (2016) for intestinal and colorectal tumors in $APC^{1638N/+}$ male and female mice.

Radiation type	LET, keV/μm	α, Gy^{-1}	RBE	α, Gy^{-1}	RBE
		Intestinal tumors, Males		**Intestinal tumor, Females**	
γ-rays	**–**	3.45 ± 0.28	–	3.07 ± 0.76	–
^{12}C (290 MeV/u)	13	5.61 ± 1.7	1.63 ± 0.51	4.40 ± 0.66	1.43 ± 0.41
^{28}Si (300 MeV/u)	70	22.0 ± 3.8	6.4 ± 1.2	11.2 ± 4.4	3.65 ± 1.69
^{56}Fe (1000 MeV/u)	150	12.7 ± 2.8	3.68 ± 0.86	10.58 ± 2.2	3.45 ± 1.11
		Colorectal tumors, Males		**Colorectal tumors, Females**	
γ-rays	–	0.10 ± 0.02	–	–	–
^{12}C (290 MeV/u)	13	0.58 ± 0.28	5.80 ± 3.03 *(5.8 ± 4.2)**	0.21 ± 0.04	∞ *(2.8 ± 1.9)**
^{28}Si (300 MeV/u)	70	1.50 ± 0.51	15.0 ± 5.92 *(15.0 ± 9.7)*	0.71 ± 0.28	∞ *(9.5 ± 7.3)*
^{56}Fe (1000 MeV/u)	150	1.19 ± 0.60	11.9 ± 6.45 *(11.9 ± 8.9)*	0.74 ± 0.41	∞ *(9.9 ± 8.6)*

**For Si and Fe only 0, 0.1, and 0.5 Gy data are used due to downward curvature expected at higher doses.
* RBE estimate as ratio of initial slope, α for particle over γ-ray tumor frequency at 2 Gy normalized to per unit dose.

Table 3
Relative biological effectiveness (RBE) factors against acute γ-rays for solid tumors estimate and track structure radiation quality factor parameter, Σ_0/α_γ estimated from mouse experiments with heavy ion or fission neutron irradiations.

Tumor type	Mouse strain	Sex	Radiation, LET (keV/μm) (Energy, MeV/u)	$RBE_{\gamma Acute}$	Σ_0/α_γ, μm^2 Gy
Harderian gland	B6CF1	F	Global Fit	–	635.2 ± 172
Lung	B6CF1	F	^{28}Si, 70 (260)	1.56 ± 1.29	468.2 ± 533.4
			^{48}Ti, 100 (1000)	3.74 ± 1.33	1302.7 ± 575.5
			^{56}Fe, 193 (600)	4.49 ± 2.67	1485.4 ± 946.1
Intestinal	$APC^{1638N/+}$	F	^{28}Si, 69 (300)	3.65 ± 1.69	1564 ± 900
			^{56}Fe, 148 (1000)	3.45 ± 1.11	1079 ± 412.5
Colorectal	$APC^{1638N/+}$	F	^{28}Si, 69 (300)	9.47 ± 7.33	4393 ± 3711
			^{56}Fe, 148 (1000)	9.87 ± 8.55	3270 ± 2962
All epithelial	B6CF1	F	Fission neutron	11.00 ± 1.60	2746 ± 399.4
Lung	B6CF1	F	Fission neutron	10.30 ± 2.20	2558 ± 546.3
Liver	B6CF1	F	Fission neutron	4.40 ± 1.60	969 ± 353
Glandular and Reproductive organs excluding ovarian	B6CF1	F	Fission neutron	7.40 ± 1.00	1777 ± 240.1
Harderian gland	B6CF1	F	Fission neutron	5.80 ± 1.20	1346 ± 278.6
Lung	BALB/c	F	Fission neutron	11.80 ± 2.95	2961 ± 740.3
Mammary	BALB/c	F	Fission neutron	9.70 ± 2.43	2396 ± 599
Pituitary	RFM	F	Fission neutron	22.50 ± 5.63	5842 ± 1460
Harderian gland	RFM	F	Fission neutron	14.6 ± 3.65	3715 ± 928.3
Intestinal	$APC^{1638N/+}$	M	^{28}Si, 69 (300)	6.37 ± 1.22	2885 ± 898.5
			^{56}Fe, 148 (1000)	3.68 ± 0.86	1159 ± 342
Colorectal	$APC^{1638N/+}$	M	^{28}Si, 69 (300)	15.00 ± 9.70	7082 ± 5002
			^{56}Fe, 148 (1000)	11.90 ± 8.88	3963 ± 3092
Hepatocellular carcinoma	CBA	M	^{56}Fe, 150 (1000)	48.98 ± 22.11	16,838 ± 8099
Hepatocellular carcinoma	C3H	M	^{28}Si, 64 (300)	81.69 ± 65.73	36,635 ± 30,878
			^{56}Fe, 181 (600)	74.31 ± 58.63	24,160 ± 19,381
All epithelial	B6CF1	M	Fission neutron	12.10 ± 4.50	3042 + 1131
Lung	B6CF1	M	Fission neutron	11.00 ± 2.00	2746 ± 499
Liver	B6CF1	M	Fission neutron	19.30 ± 5.60	4980 ± 1445
Glandular and Reproductive organs excluding ovarian	B6CF1	M	Fission neutron	16.60 ± 5.60	4253 ± 1435
Harderian gland	B6CF1	M	Fission neutron	12.10 ± 2.90	3042 ± 729

In Eqs. (7) and (8) the maximum RBE occurs when P∼2/3 and the classic over-kill effect leading to decreasing RBE's for P > 2/3.

Table 3 shows estimates of (Σ_0/α_γ) for various solid tumors in mice following fission neutron (Ullrich et al., 1976; Ullrich and Storer, 1979; Ullrich 1983; Ullrich, 1984; Grahn et al., 1992) and heavy ion irradiation (Fry et al., 1985; Alpen et al., 1993; Chang et al., 2016; Chang and Blakely, 2016; Weil et al., 2009; 2014; Suman et al., 2016) using the approach described in the Method section. A large tumor type and mouse strain specific dependence is observed, while large statistical uncertainties occur for several of the experiments. A recent study by Wang et al. (2015) finds a relative effectiveness at a dose of 1 Gy of heavy ions to γ-rays of about 7 using male and female C57BL/6 mice, however detailed dose response data were not made to estimate RBE.

It is important to note that the fission neutron experiments in Table 3 were made using chronic irradiation, while the more recent heavy ion experiments were carried out with acute irradiation at modest dose values. One comparison that can be made more directly is for Harderian gland tumors in B6CF1 mice were we find values for Σ_0/α_γ of 1346 ± 278.6 and 635.2 ± 172 for chronic fission neutron irradiation (Grahn et al., 1992) and a global fit to several low dose heavy ion exposures (Cucinotta and Cacao, 2016), respectively. However other differences in the experimental design occurred, including lifespan versus prevalence at 600 d, and the use of pituitary isografts as a tumor promoter with head only irradiation by Fry et al. (1985) and Alpen et al. (1993) but not Chang et al. (2016). Also the global fit (Cucinotta and Cacao, 2016) makes corrections for cell sterilization effects.

Fig. 3 **(panel A)** shows the resulting cumulative distribution function (CDF) of values of Σ_0/α_γ that results from these experiments, which show that most values are contained within a 3-fold variation above or below the median value. For high LET particles, the QF value limits to the value of (Σ_0/α_γ)/LET when P∼1 as seen from Eq. (6). For evaluating the CDF a few experiments used multiple irradiation types and here we averaged the estimates such that only one data point is counted towards the CDF, with the ex-

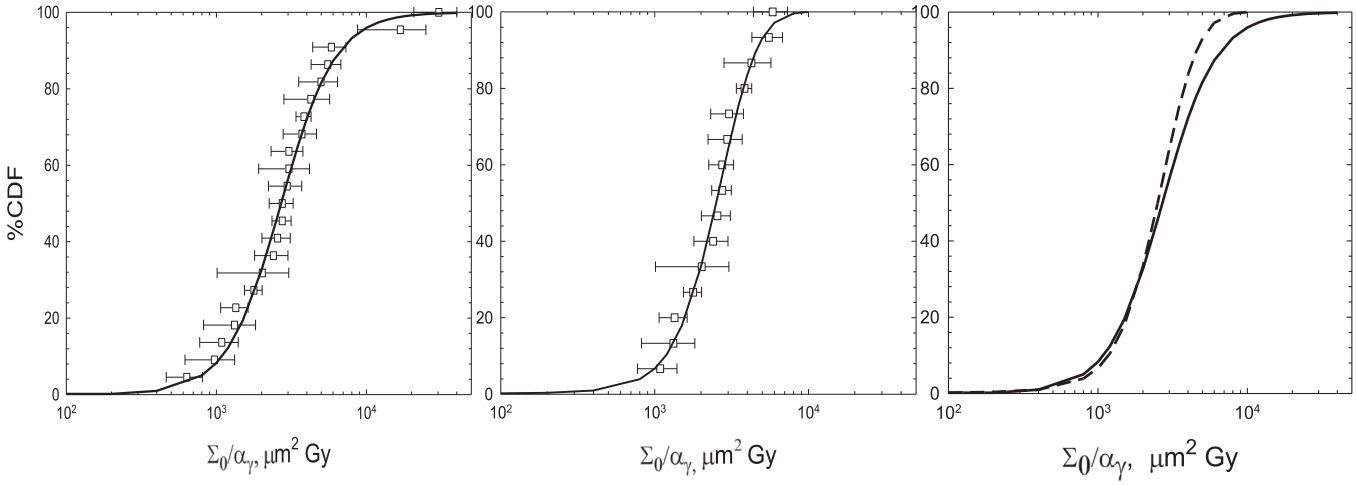

Fig. 3. Cumulative distribution functions (CDF) of track structure quality factor function parameter, Σ_0/α_γ , from mouse solid tumor data for heavy ions and fission neutrons described in text. Right panel results for all data with logistic function fit described in Table 4. Center panel solid tumor data excluding studies of liver and Harderian gland tumors and Gompertz function fit. Right panel compares resulting fits of CDFs in left and center panels.

ception of the heavy ion experiments for Harderian gland tumors were a global fit to 10 particle types was used to obtain the value of (Σ_0/α_γ) (Cucinotta and Cacao, 2016). The experiments of Weil et al. (2009,2014) for hepatocellular carcinoma in CBA and C3H mouse irradiations with heavy ions leads to a highly skewed distribution to large (Σ_0/α_γ) values. Statistical uncertainties are more prominent in the more recent heavy ion experiments compared to fission neutron studies; however the results of Table 3 suggest tissue dependent factors are of major importance and should be further investigated.

It should be noted that distinct mechanisms for tumor induction for low energy protons produced by fission neutrons, with narrow high density track structures, compared to high energy heavy ions, with significant track core and penumbra, are possible, but little is known in this area. For all experiments combined higher mean values of (Σ_0/α_γ) are found for heavy ion alone, $(7707 \pm 350.2)/6.24$ compared to fission neutron experiments alone, $(3027 \pm 879)/6.24$. This difference is largely due to the large values found for hepatocellular carcinomas in heavy ion irradiation as mean values are more similar with this tumor type removed, $(2403 \pm 2277)/6.24$ and $(3096 \pm 934)/6.24$) for heavy ions and fissions neutrons, respectively. Differences in tumor types and mouse strains confound a conclusion on which radiation type is more carcinogenic, while the track structure model predicts monoenergetic protons of about 0.3 MeV are more carcinogenic per unit dose than heavy ions of any energy.

3.2.1. Parameter estimates for liver cancer risks

RBEs for hepatocellular carcinoma for heavy ions in both male C3H and CBA mice are reported (Weil et al., 2009; 2014) as several times higher than other tumor types (Dicello et al., 2004; Fry et al., 1985; Alpen et al., 1993; Chang et al., 2016; Suman et al., 2016). Ullrich did not observe a significant number of liver cancers in female Balb/c or RFM mice (Ullrich, 1983; Ullrich et al., 1976) exposed to γ-rays or fission neutrons. In contrast large RBE's were reported for liver cancers in B6CF1 male mice in the studies of Grahn et al. (1992) and Takashi et al. (1992). Both studies found larger RBE values for male compared to female mice. In Table 3 we used RBE values from Grahn et al. (1992) for chronic fission neutron irradiations of 24 weeks; however Takashi et al. (1992) found similar differences in RBE's for acute fission neutron exposures in males and females of 15.2 and 2.5, respectively. No studies of RBE's for hepatocellular carcinomas in female mice exposed to heavy ions have been reported. The above observations suggest important genetic and sex dependencies to liver cancer risk, which impact RBE estimates.

The LSS study of atomic-bomb survivors in Japan is the main source of data for risk estimates from low LET radiation. As noted by Preston et al. (2007), the incidence of liver cancer is much higher in Japan than in the US, with world-population age standardized incidence rates of 23.5 and 7.5 per 100,000 for Japanese men and women, respectively compared to the U.S. white and European rates, which range from 3 to 12 for men and from 1 to 5 for women. Liver cancer subtypes include hepatocellular carcinoma, cholangiocarcinoma (bile duct cancer), hepatoblastoma, and angiosarcoma, while hepatocellular carcinoma accounts for most of the larger incidence observed in the Japanese compared to the U.S. population. Baseline liver cancer rates are higher for males compared to females in both countries. Major risk factors for liver cancer are chronic infection with hepatitis B or C virus, dietary exposure to aflatoxins, chronic alcohol consumption, and tobacco smoking. A significant interaction between radiation hepatocellular carcinoma risk and hepatitis C infection is observed in the LSS study (Sharp et al., 2003). Astronauts are reported to have low incidence rates of tobacco use, alcoholism, and hepatitis B or C infection, suggesting lower background rates for liver cancer risk compared to the U.S. population. The use of the multiplicative risk model in Eq. (2) accounts for part of the differences expected between model populations, however other differences related to healthy worker effects are important considerations.

Cologne et al. (1999) reported that male atomic-bomb survivors exposed as teenagers or in their 20s had a significantly increased risk of liver cancer, while a small radiation risk occurred for males of older ages or females of all ages of exposure. This could indicate a biological mechanism in young adult males or a birth cohort effect. Astronauts on ISS or exploration missions would generally be above age 40 y at the time of mission. Hepatocellular carcinoma dominated the excess liver cancer risk in the Atomic-bomb survivors. In a study of thorotrast patients in Western countries, cholangiocarcinoma and hepatoblastoma dominated excess risk (Travis et al., 2003), however the radioisotope deposits in connective tissue perhaps reducing the risk of hepatocellular carcinoma (NAS, 2006). We could not find any RBE values for cholangiocarcinoma and hepatoblastoma in the scientific literature, and they would be difficult to study in mice where hepatocellular carcinomas dominate.

Table 4
Cumulative distribution function (CDF) for model parameter (Σ_0/α_γ) determined by fits to data for heavy ions and fission neutrons*. Means and fits of CDF corresponding to values of Table 3 using logistic or Gompertz equations are shown with best fit shown in bold font.

Data sets	Mean, μm^2 Gy	A	B, μm^2 Gy	C	Adj R2
All solid cancer data	(4728 ± 1378)/6.24				
Logistic Equation Fit		**1.0 ± 0.027**	**(2699 ± 87)/6.24**	**-2.42 ± 0.16**	**0.997**
Gompertz Equation Fit		1.0 ± 0.02	(2195 ± 55.2)/6.24	(1551 ± 84.8)/6.24	0.987
Solid cancer excluding liver, and Harderian gland tumors	(2897 ± 357)/6.24				
Logistic Equation Fit		1.0 ± 0.053	(2483 ± 110)/6.24	-3.26 ± 0.39	0.974
Gompertz Equation Fit		**1.0 ± 0.039**	**(2104 ± 68.7)/6.24**	**(1109 ± 110)/6.24**	**0.979**
Lung	(2338 ± 905)/6.24				
Liver	(13,296 ± 4739)/6.24				

*Parameters that result from fits of the logistic equation, CDF=A/[1 +((Σ$_0$/α$_\gamma$)/B)^C] or Gompertz equation CDF=Aexp[-exp(-Σ$_0$/α$_\gamma$ –B)/C] to data for (Σ$_0$/α$_\gamma$) from mouse experiments for heavy ions and fission neutrons shown in Table 3.

Table 5
Predictions of risk of exposure induced death (REID) and 95% confidence intervals for 1-year space missions at average solar minimum for 45-year old never-smoker females with several models of the uncertainty distribution for the dose and dose-rate reduction effectiveness factor (DDREF). REID(Total) includes cancer and circulatory diseases.

Mission and Model	%REID (Cancer)	%REID (Total)
	1-Year ISS Missions	
DDREF Model A	0.94 [0.18, 3.0]	1.26 [0.36, 3.28]
DDREF Model B	0.86 [0.16, 2.83]	1.18 [0.34, 3.09]
DDREF Radiobiology data	0.81 [0.14, 2.79]	1.13 [0.33, 3.08]
	1-Year Deep Space Missions	
DDREF Model A	1.88 [0.36, 6.16]	2.52 [0.71, 6.74]
DDREF Model B	1.75 [0.31, 6.03]	2.4 [0.68, 6.61]
DDREF Radiobiology data	1.66 [0.28, 5.89]	2.31 [0.64, 6.41]

Because of the above considerations we pursued an alternate analysis separating out liver cancer from the overall solid cancer CDF as shown in Table 4 and Fig. 3 **(Panel B)**. For this comparison we also removed the Harderian gland values because this gland does not occur in humans, however note the use of the Harderian gland data for the QF shape parameters (m and κ) is needed because no other data sets have been reported to estimate these parameters. Fig. 3 **(Panel C)** compares the resulting distributions for all data and excluding liver and Harderian gland values. We also show values for lung cancer risk; the only other tissue site were multiple measurements of RBE's has been reported for different mouse strains and high LET radiation types. These results suggest QFs for liver cancer in males could be significantly larger than other cancer types. The lung cancer value in Table 4 is lower than the overall average but not significantly, which is not surprising since lung cancer dominates overall radiation risks.

3.3. Space mission risk predictions

We next used the revised methods to make predictions for one-year missions for average solar minimum conditions in deep space or aboard the ISS, and a 940 day Mars mission. Predictions are made with different model assumptions for 45-year old male and female never-smokers assuming a heavily shielded Mars transfer spacecraft (20 g/cm^2 aluminum) and a lighter Mars surface habitat (10 g/cm^2). Comparisons for other ages, solar cycle conditions including solar particle events (SPE), and shielding values can be made using this approach as have been reported in previous analysis (Cucinotta et al., 2013a; Cucinotta 2014).

We first considered a sensitivity analysis of several of the model assumptions related to the PDF of the DDREF and QF parameter, Σ_0/α_γ, uncertainties. In Table 5 we show comparisons for 1-year ISS and deep space missions for 45-y old never-smoker (NS) females using the DDREF Models A and B, and the likelihood function for the combined mouse solid tumor and proton radiobiology studies of dose-rate. These results show that only modest changes in risk predictions (on the order of 10%) for different DDREF assumptions are found in the most recent formation of the NASA QF where the track core term is assumed not to be influenced by dose-rate effects. Larger changes are predicted for SPE exposures and will be reported elsewhere. Also shown in Table 5 are predictions of the circulatory disease contributions to the total REID, which contributed about 25% for females when applying the meta-analysis results of Little et al. (2012) as described previously (Cucinotta et al., 2013b). In Table 6 we compared predictions for 1-year deep space missions for 45-y old NS males using different assumptions for the CDF of uncertainty for the QF parameter Σ_0/α_γ. Here mean risk predictions and upper 95% confidence levels are reduced by about 12% and 30%, respectively when the values for hepatocellular carcinomas representing liver cancer and Harderian gland tumors are excluded from the CDF of uncertainty. Table 6 also shows estimates of liver cancer REIC where the mouse hepatocellular carcinomas are applied directly to this tissue type in the model. Here the REID prediction is increased almost 3-fold compared to using the average overall CDF from all available experiments. Because of the risk factors observed in the LSS studies and the healthy worker attributes expected for astronauts as discussed above, we recommend that the CDF for the reduced set of data be used for mission risk predictions, while the more conservative estimate for male liver cancer risk be considered as a separate calculation.

Using our preferred models we next considered risk predictions for a 940 d Mars mission with 400 day transit time and 540 days on the Martian surface. Fig. 4 shows predictions of tissue specific REIC, and total cancer REIC and REID along with predictions for CVD and IHD. Circulatory disease risks comprise 25% and 40% of the total REID for females (lower panel) and males (upper panel), respectively. Lung cancer risks are the dominate risk for females and show a large uncertainty due to large differences in the additive and multiplicative transfer models, while IHD is similar to lung cancer risk for males. The predictions of mean and 95% CI for a Mars mission are above NASA safety standards for males and females.

4. Conclusions

Based on the current and previous analysis (Cucinotta et al., 2013a; NRC, 2013; NCRP 2014; Cucinotta 2015) the uncertainties in the physics of organ doses and particle spectra, transfer model, the DDREF, and m and κ parameters are roughly equal in the current approach with only modest changes to risk predictions associated with uncertainties in each factor (< 25%). However the available data on surrogate cancer endpoints is limited to a few endpoints such as chromosomal aberrations, gene mutation and neoplastic transformation, and there is a need to develop data bases at low

Table 6
Predictions of risk of exposure induced cancer (REIC) or death (REID) and 95% confidence intervals for 1-year deep space missions at average solar minimum for 45-year old never-smoker males with several models of the quality factor parameter, (Σ_0/α_γ) and its uncertainty distribution from Table 4. REID(Total) includes cancer and circulatory disease fatalities. Risks of exposure induced cancers (REIC) for liver risk under different QF parameter assumptions are also shown.

Model	%REIC (Cancer)	%REID (Cancer)	%REID (Total)
Σ_0/α_γ estimate based on all solid cancer experiments	2.23 [0.53, 7.84]	1.3 [0.23, 4.73]	2.16 [0.86, 5.59]
Σ_0/α_γ estimate excludes liver & Harderian gland data	1.96 [0.53, 5.83]	1.1 [0.21, 3.36]	1.97 [0.86, 4.26]
	Liver Cancer		
Σ_0/α_γ estimate based on all solid cancer experiments	0.13 [0.02, 0.48]		
Σ_0/α_γ direct estimate from mouse liver data	0.37 [0.05, 1.41]		

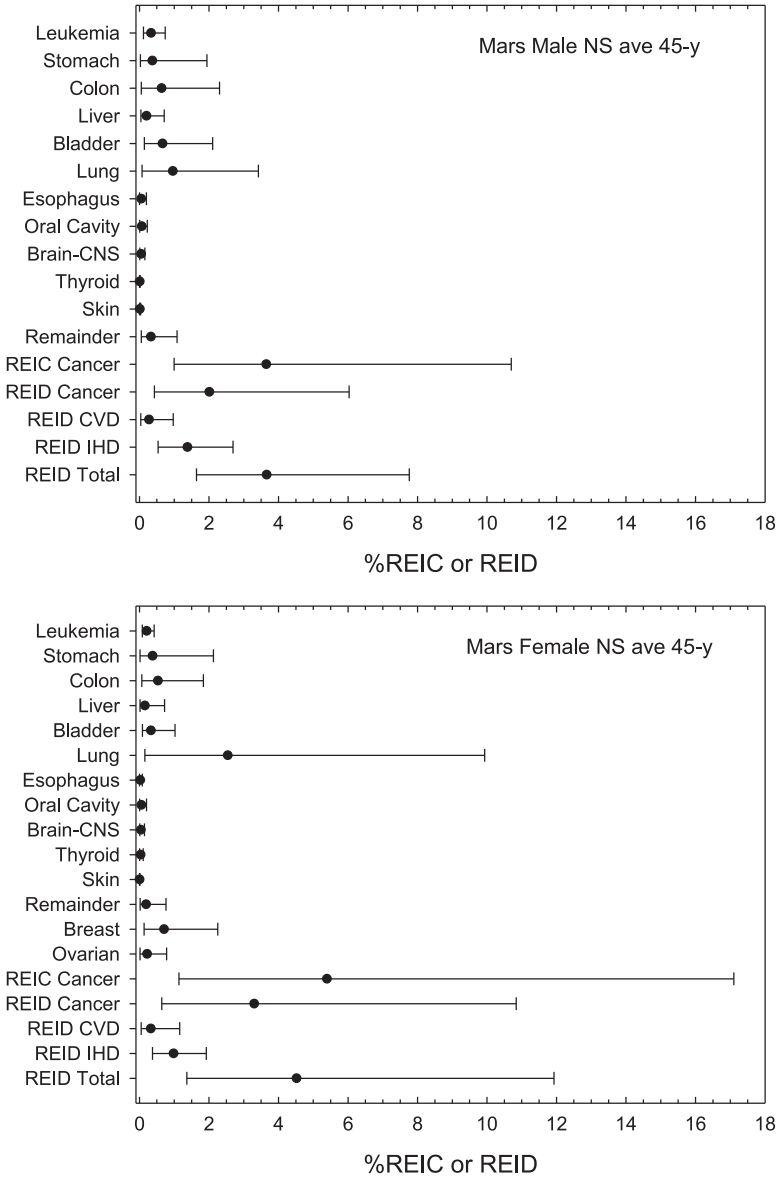

Fig. 4. Predictions of tissue specific risk of exposure induced cancer (REIC) and risk of exposure induced death (REID) for 45-y old male (upper panel) or females (lower panel) for a Mars mission. Predictions assume average solar minimum galactic cosmic ray environment for 20 g/cm^2 aluminum shielding using Model B for dose-rate effects and quality factor parameters described in main text. Predictions of cardiovascular disease (CVD) and ischemic heart disease (IHD) risks are also shown.

dose with multiple particle types for other surrogate endpoints of cancer risk. Uncertainties with higher impact are the potential role of more lethal tumors observed for high LET radiation compared to spontaneous or low LET induced tumors as suggested by mouse experiments (Grahn et al., 1992; Imaoka et al., 2007; Weil et al., 2014; Illa-Bochaca et al., 2014; Wang et al., 2015; Cucinotta et al., 2015), and the uncertainty in the values of Σ_0/α_γ, either of which can influence risk predictions by more than 50%. Of note is that the lack of detailed low dose and radiation quality study of tumors for other tissues besides the Harderian gland, whereupon if such data were obtained it could potential modify the uncertainty in the m and κ parameters, as well as estimates of Σ_0/α_γ. Beyond these uncertainties the role of non-targeted effects (NTE) could increase risk predictions by an even larger amount, with a recent estimate suggesting an GCR averaged RBE as high as 10 compared to < 5 for targeted effects models (Cucinotta and Cacao, 2016). Furthermore, the pros and cons in the use of mouse models for human risk estimates (Fry, 1995) should continue to be evaluated, while there is a vital need to develop and validate more accurate experimental models of human cancer risks than used in the past and to develop the mechanistic understanding of why large tissue, sex, and genetic dependent variations in high LET cancer risks occur.

Acknowledgments

This study was supported by the University of Nevada, Las Vegas and the Nevada Undergraduate Idea Network of Biomedical Research Institute (INRBE). We are grateful to Paula Bennett for sending raw data from experiments she performed with Dr. Betsy Sutherland on proton dose-rate effects, and to Ellie Blakely and Polly Chang for discussions on tumor types observed in their recent experiments.

References

Alpen, EL, Powers-Risius, P, Curtis, SB, DeGuzman, R, 1993. Tumorigenic potential of high-Z, high-LET charged particle radiations. Radiat. Res. 88, 132–143.
Barkas, H, 1963. Nuclear Research Emulsions. Academic Press Inc, New York Vol. 1, Chap. 9, p. 371.
Belli, M, Goodhead, DT, Ianzini, F, Simone, G, Tabocchini, MA, 1992. Direct comparison of biological effectiveness of protons and alpha-particles of the same LET. II. Mutation induction at the HPRT locus in V79 cells. Int. J. Radiat. Biol. 61, 625–629.
Boice, JD, 1993. Leukemia risk in thorotrast patients. Radiat. Res. 136, 301–302.
Cacao, E, Hada, M, Saganti, PB, George, KA, Cucinotta, FA, 2016. Relative biological effectiveness of HZE particles for chromosomal exchanges and other surrogate cancer risk endpoints. PLoS One 11 (4), e0153998.
CDC, Centers for disease control and prevention, national center for health statistics. Multiple cause of death 1999-2014 on CDC WONDER online database, released 2015. Data are from the Multiple Cause of Death Files, 1999-2014, as compiled from data provided by the 57 vital statistics jurisdictions through the Vital Statistics Cooperative Program.
Chang, PY, Cucinotta, FA, Bjornstad, KA, Bakke, J, Rosen, CJ, Du, N, Fairchild, DG, Cacao, E, Blakely, EA, 2016. Harderian gland tumorigenesis: low-dose and LET response. Radiat. Res. 185, 449–460.
Chang PY, Blakely EB, 2016. Particle radiation-induced lung tumors: dose and LET-dependence. To be submitted.
Chylack, LT, Peterson, LE, Feiveson, A, Wear, M, Manuel, FK, Tung, WH, Hardy, DS, Marak, LJ, Cucinotta, FA, 2009. NASCA report 1: cross-sectional study of relationship of exposure to space radiation and risk of lens opacity. Radiat. Res. 172, 10–20.
Clapp, NK, Darden, EB, Jr, JerniganMC, 1974. Relative effects of whole-body sublethal doses of 60-MeV protons and 300-kVp X-rays on disease incidence in RF mice. Radiat. Res. 57, 158–186.
Cologne, JB, Tokuoka, S, Beebe, GW, Fukuhara, T, Mabuchi, K, 1999. Effect of radiation on incidence of primary liver cancer among atomic bomb survivors. Radiat. Res. 152, 364–373.
Cucinotta, FA, Manuel, F, Jones, J, Izsard, G, Murray, J, Djojonegoro, B, Wear, M, 2001. Space radiation and cataracts in astronauts. Radiat. Res. 156, 460–466.
Cucinotta FA, Kim MY, Chappell L, 2013a. Space radiation cancer risk projections and uncertainties- 2012. NASA TP 2013–217375.
Cucinotta, FA, Kim, MY, Chappell, LJ, Huff, JL, 2013b. How safe is safe enough: radiation risks for a human mission to Mars. PLoS One 8 (10), e74988.
Cucinotta, FA, 2014. Space radiation risks for astronauts on multiple international space station missions. PLoS One 9 (4), e96099.
Cucinotta, FA, 2015. A new approach to reduce uncertainties in space radiation cancer risk predictions. PLoS One 10 (3), e0120717.
Cucinotta, FA, Alp, M, Rowedder, B, Kim, MY, 2015. Safe days in space with acceptable uncertainty from space radiation exposure. Life Sci. Space Res. 5, 54–69.
Cucinotta, FA, Hamada, N, Little, MP, 2016a. No evidence of an increase in circulatory disease mortality in astronauts following space radiation exposures. Life Sci. Space Res. 10, 53–56.
Cucinotta, FA, Cacao, E, Alp, M, 2016b. Space radiation quality factors and the delta-ray dose and dose-rate reduction effectiveness factor. Health Phys. 110, 262–266.
Cucinotta FA, Cacao E, 2016. Do non-targeted effects in galactic cosmic ray exposures significantly increase astronaut cancer risk for a Mars mission? Submitted.
Cullings, HM, Pierce, DA, Kellerer, AM, 2014. Accounting for neutron exposure in the Japanese atomic bomb survivors. Radiat. Res. 182, 587–598.
DevCan: Probability of developing or dying of cancer software, version 6.2.0. statistical research and applications branch, national cancer institute, 2007. Accessed June 1, 2016.
Dicello, JF, Christian, A, Cucinotta, FA, Gridley, DS, Kathirithhamby, R, Mann, J, et al., 2004. *In vivo* mammary tumorigenesis in the Sprague-Dawley rat and microdosimetric correlates. Phys. Med. Biol. 49, 3817–3830.
Edwards, AA, Dennis, JA, 1975. The calculation of charged particle fluence and LET spectra for the irradiation of biologically significant materials by neutrons. Phys. Med. Biol. 20, 395–409.
Ellender, M, Harrison, JD, Meijne, E, Huiskamp, R, Kozlowski, RE, Haines, JW, et al., 2011. Intestinal tumours induced in Apc $^{Min/+}$ mice by X-rays and neutrons. Int. J. Radiat. Biol. 87, 385–399.
Fry, RJM, Powers-Risius, P, Alpen, EL, Ainsworth, EJ, 1985. High LET radiation carcinogenesis. Radiat. Res. 104, S188–S195.
Fry RJM, 1995. Mice, Myths, and Men. National Council on Radiation Protection and Measurements, Lauriston S. Taylor Lectures in Radiation Protection and Measurements, Lecture No 18 . Bethesda MD.
George, K, Willingham, V, Wu, H, Gridley, D, Nelson, G, Cucinotta, FA, 2002. Chromosome aberrations in human lymphocytes induced by 250 MeV protons: effects of dose, dose rate and shielding. Adv. Space Res. 30, 891–899.
Grahn, D, Lombard, LS, Carnes, BA, 1992. The comparative tumorigenic effects of fission neutrons and Cobalt-60 γ rays in B6CF$_1$ mouse. Radiat. Res. 129, 19–36.
Hoel, DG, 2015. Comments on the DDREF estimate of the BEIR VII committee. Health Phys. 108, 351–356.
Hunter, N, Charles, MW, 2002. The impact of possible modifications to the DS86 dosimetry on neutron risk and relative biological effectiveness. J. Radiol. Prot. 22, 357–370.
Illa-Bochaca, I, Ouyang, H, Tang, J, Sebastiano, C, Mao, JH, Costes, SV, et al., 2014. Densely ionizing radiation acts via the microenvironment to promote aggressive Trp53 null mammary carcinomas. Cancer Res. 74, 7137–7148.
Imaoka, T, Nishimura, KakinumaS, Hatano, Y, Ohmachi, Y, Yoshinaga, S, et al., 2007. High relative biological effectiveness of carbon ion irradiation on induction of rat mammary carcinoma and its lack of H-ras and Tp53 mutations. Int. J. Radiat. Oncol. Biophys. 69, 194–203.
ICRP, Recommendations of the International Commission on Radiological Protection, ICRP Publication 103; Ann. ICRP 37, (2–4); 2007.
Jenkins, SP, 2013. LOGNFIT: stata module to fit lognormal distribution by maximum likelihood. Statistical Software Components. Boston College Department of Economics http://EconPapers.repec.org/RePEc:boc:bocode:s456824.
Katz, R, Ackerson, B, Homayoonfar, M, Scharma, SC, 1971. Inactivation of cells by heavy ion bombardment. Radiat. Res. 47, 402–425.
Kronenberg, A, Gauny, S, Kwoh, E, Grossi, G, Dan, C, Grygoryev, D, et al., 2013. Comparative analysis of cell killing and autosomal mutation in mouse kidney epithelium exposed to 1 GeV protons in vitro or in vivo. Radiat. Res. 179, 511–520.
Little, MP, 1997. Estimates of neutron relative biological effectiveness derived from the Japanese atomic bomb survivors. Int. J. Radiat. Biol. 72, 715–726.
Little, MP, Azizova, TV, Bazyka, D, Bouffler, SD, Cardis, E, Chekin, S, et al., 2012. Systematic review and meta-analysis of circulatory disease from exposure to low-level ionizing radiation and estimates of potential population mortality risks. Environ. Health Perspect. 120, 1503–1511.
Miller, RC, Hall, EJ, 1991. Oncogenic transformation of C3H 10T1/2 cells by acute and protracted exposures to monoenergetic neutrons. Radiat. Res. 128, S60–S64.
NAS (National Academy of Sciences Space Science Board), 1996. Report of the Task Group on the Biological Effects of Space Radiation: Radiation Hazards to Crews on Interplanetary Missions. The National Academies Press, Washington DC.
NAS, BEIRVII., 2006. Health risks from exposure to low levels of ionizing radiation. National Academy of Sciences Committee on the Biological Effects of Radiation. National Academy of Sciences Press, Washington D.C.
NCRP, 1997. Uncertainties in fatal cancer risk estimates used in radiation protection. National Council on Radiation Protection and Measurements NCRP Report No. 126: Bethesda MD.
NCRP, 2000. Recommendations of dose limits for low Earth orbit. National Council on Radiation Protection and Measurements Report 132: Bethesda MD.
NCRP, 2006. Information needed to make radiation protection recommendations for space missions beyond low-Earth orbit. National Council on Radiation Protection and Measurements Report No. 153: Bethesda MD.
NCRP. Radiation protection for space activities: supplement to previous recommendations. National Council on Radiation Protection and Measurements Commentary 23: Bethesda MD; 2014.

NIST, 2009. Stopping-power and range tables for electrons, protons, and helium ions. National Institute of Standards and Technology Report NISTIR 4999; Gaithersburg MD.

NRC, 2013. Technical evaluation of the NASA model for cancer risk to astronauts due to space radiation. National Research Council. The National Academies Press, Washington DC.

Pandita, T, Geard, CR, 1996. Chromosome aberrations in human fibroblasts induced by monoenergetic neutrons. I. Relative biological effectiveness. Radiat. Res. 145, 730–739.

Peng, Y, Hatsumi, N, Warner, C, Bedford, JS, 2012. Genetic susceptibility: radiation effects relevant to space travel. Health Phys. 103, 607–620.

Preston, DL, Ron, E, Tokuoka, S, Funamota, S, Nishi, N, Soda, M, et al., 2007. Solid cancer incidence in atomic bomb survivors:. Radiat. Res. 168, 1958–1998 1-64.

SEER, 2015. Surveillance, epidemiology, and end results (SEER) program (www.seer.cancer.gov) DevCan database. SEER 18 Incidence and Mortality, 2000-2012, With Kaposi Sarcoma and Mesothelioma National Cancer Institute, DCCPS, Surveillance Research Program, Cancer Statistics Branch, released April-based on the November 2014 submission. Underlying mortality data provided by NCHS (www.cdc.gov/nchs).

Sharp, GB, Mizuno, T, Cologne, JB, Fukuhara, T, Fujiwara, S, Tokuoka, S, Mabuchi, K, 2003. Hepatocellular carcinoma among atomic bomb survivors: significant interaction of radiation with hepatitis C virus infections. Int. J. Cancer 103, 531–537.

Stisova, V, Abele, WA, Thompson, KH, Bennett, PV, Sutherland, BM, 2011. Response of primary human fibroblasts exposed to solar particle event protons. Radiat. Res. 176, 217–225.

Suman, S, Kumar, S, Moon, BH, Strawn, SJ, Thakor, H, Fan, Z, Shay, JW, Fornace Jr, AJ, Datta, K, 2016. Relative biological effectiveness of energetic heavy ions for intestinal tumorigenesis shows male preponderance and radiation type and energy dependence in APC$^{1638N/+}$ mice. Int. J. Radiat. Oncol. Biol. Phys. 95, 131–138.

Takashi, T, Watanabe, H, Dohi, K, Ito, A, 1992. ^{252}Cf relative biological effectiveness and inheritable effect of fission neutrons in mouse liver tumorigenesis. Cancer Res. 52, 1948–1952.

Tanaka, K, Gajendiran, N, Endo, S, Komatsu, K, Hoshi, M, Kamada, N, 1999. Neutron energy-dependent initial DNA damage and chromosomal exchange. J. Radiat. Res. 40, S36–S44.

Thacker, J, Stretch, A, Stephens, MA, 1979. Mutation and inactivation of cultured mammalian cells exposed to beams of accelerated heavy ions. II. Chinese hamster V79 cells. Int. J. Radiat. Biol. 38, 137–148.

Tracy, BL, Stevens, DL, Goodhead, DT, Hill, MA, 2015. Variation in RBE for survival of V79-4 cells as a function of alpha-particle (helium ion) energy. Radiat. Res. 184, 33–45.

Travis, L, Hauptmann, M, Knudson Gaul, L, Storm, HH, Goldman, MB, Nyberg, U, et al., 2003. Site-specific cancer incidence and mortality after cerebral angiography with radioactive thorotrast. Radiat. Res. 160, 690–706.

Ullrich RL, Jernigan MC, Cosgrove GE, Satterfield LC, Bowles ND, Storer JB, 1976. The influence of dose and dose rate on the incidence of neoplastic disease in RFM mice after neutron irradiation. Radiat. Res.. 68, 115–131.

Ullrich, RL, Storer, JB, 1979. Influence of γ irradiation on the development of neoplastic disease in mice: I. Reticular tissue tumors. Radiat. Res. 80, 303–316.

Ullrich, RL, 1983. Tumor induction in BALB/c female mice after fission neutron or γ irradiation. Radiat. Res. 83, 506–515.

Ullrich, RL, 1984. Tumor induction in BALB/c mice after fractionated or protracted exposures to fission-spectrum neutrons. Radiat. Res. 97, 587–597.

Ullrich, RL, Preston, RJ, 1987. Myeloid leukemia in male RFM mice following irradiation with fission spectrum neutrons or γ-rays. Radiat. Res. 109, 165–170.

United Nations Scientific Committee on the Effects of Atomic Radiation, 2008. Sources and Effects of Ionizing Radiation UNSCEAR 2006 Report to the General assembly, With Scientific Annexes. United Nations;, New York.

Walsh, L, 2013. Neutron relative biological effectiveness for solid cancer incidence in the Japanese A-bomb survivors – an analysis considering the degree of independent effects from γ-ray and neutron absorbed doses with hierarchical partitioning. Radiat. Environ. Biophys. 52 (1), 29–36.

Wang, X., Farris, AB, Wang, P, Zhang, X, Wang, H, Wang, Y, 2015. Relative effectiveness at 1 Gy after acute and fractionated exposures of heavy ions with different linear energy transfer for lung tumorigenesis. Radiat. Res. 18, 233–239.

Weil, MM, Bedford, JS, Bielefeldt-Ohmann, H, Ray, AF, Gernik, PC, Ehrhart, EJ, et al., 2009. Incidence of acute myeloid leukemia and hepatocellular carcinoma in mice irradiated with 1 GeV/nucleon ^{56}Fe ions. Radiat. Res. 172, 213–219.

Weil, MM, Ray, FA, Genik, PC, Yu, Y, McCarthy, M, Fallgren, CM, et al., 2014. Effects of ^{28}Si ions, ^{56}Fe ions, and protons on the induction of murine acute myeloid leukemia and hepatocellular carcinoma. PLoS One 9 (8), e104819.

Wood, DH, 1991. Long-term mortality and cancer risk in irradiated rhesus monkeys. Radiat. Res. 126, 132–140.